EXPERIMENTAL RESULTS OF VESPAR SPACE RADIATOR DEVELOPMENT MODEL

Fabiano Luis de Sousa, fabiano@dem.inpe.br
Valeri V. Vlassov, vlassov@dem.inpe.br
Instituto Nacional de Pesquisas Espaciais – INPE/DMC. Av. dos Astronautas, 1758. CEP:12227-010. S.J.Campos,SP.

Adriano T. Santos, adriano_ts@yahoo.com.br
Universidade do Vale do Paraíba - UNIVAP. São José dos Campos - SP, Brazil

Abstract. In this paper, experimental results of thermal vacuum tests performed on the development model of a new concept for a space radiator with variable emittance is presented. Called VESPAR (Variable Emittance Space Radiator), this device was recently proposed as an attractive alternative to conventional thermal louvers, to be used in space applications where the spacecraft thermal control could not be accomplished satisfactorily only with use of constant emittance radiators and heaters. Numerical simulations had already shown that the VESPAR concept is feasible and experimental tests are now under way in order to experimentally verify it. This paper presents the first experimental results obtained. Thermal vacuum tests were performed to simulate three different thermal coupling states in the radiator, operating under different internal and external thermal loads conditions. The thermal loads simulate the heat dissipation of an electronic equipment coupled to the radiator and the external environment to it. The experimental results confirmed the numerical predictions that the VESPAR concept is feasible.

Keywords: Space radiator, variable emittance, spacecraft, satellite

1. INTRODUCTION

Space radiators are devices or areas on the satellite´s external surface used to exchange heat with the external environment, so that excess of heat generated inside the satellite can be rejected to space. In fact, the thermal balance in a satellite must consider the variation of internal and external heat loads, with the goal of keeping the satellite structure and equipment temperatures inside a given required range. For equipment, this range is usually from -10 to +40 ^{o}C.

Variation on the internal heat loads are due to the heat dissipation of the satellite equipment as they are turned on or off in accordance to a given satellite operational mode. For example, a remote sensing satellite in Low Earth Orbit (LEO) may turn on an imaging camera for periods of 15 minutes in a total of 100 minutes of orbit period. The same satellite will experience along the orbit different heat fluxes on its external surfaces due to the variation of direct Solar radiation, albedo (Solar radiation reflected by Earth) and Infrared radiation emmited from Earth. The variation of the external heat loads on each satellite external surface depends on the satellite´s attitude, altittude and orbit inclination.

A typical approach in satellite thermal design is to thermally insulate most of its external surfaces, while allowing certain areas, the radiators, open to reject excess heat to space. The internal heat can be transferred to these radiators by conduction or through other special thermal transfer devices such as heat pipes. Usually, in designning a space radiator, the first step is to size it to accommodate a combination of maximum internal heat loads and external fluxes, known as the hot case. Then it is verified if this design can also accomodate the cold case, when the satellite is subjected to the lowest external heat flux and equipment dissipation. If the radiator designed to the hot case leads to a temperature in the equipment below the minimum required by specification in the cold case, heaters are usually used to warm up the equipment in this condition. Although being a simple and efficient solution to overcome low temperatures in the cold case, heaters consume electrical power, a limited resource in any spacecraft. In fact, they can consume from 10 to 40 % of the total electrical power budget for maintain low-limit temperatures of equipment when the satellite is in cold case conditions.

Although using heaters to warm equipment in cold conditions means that part of the spacecraft power buget has to be dedicated to the thermal control subsystem, they are frequently used because they are simple to apply, very *low-cost* and *low-mass* devices. Nevertheless, in cases where the power budget is very limited, other types of thermal control devices can be used instead, such as thermal louvers (variable heat rejection ability), variable conductance heat pipes or thermal diodes (variable heat transport ability), as described, for example in Gilmore (1994). These devices would save power consuption but will add weight to the sattelite. Hence, there is a trade-off between power consuption, mass and reliability, that must be take into account when selecting a thermal control device for a given satellite.

One type of thermal control device used in order to avoid heaters is the thermal louver (Gilmore, 1994; Karam, 1998; Muraoka et al, 2001). It is a mechanical device that when opened expose the radiator to space, allowing internal heat from the satellite be rejected, while when closed reduces significantly the heat lost by the radiator and then protect the equipment during the cold case. The thermal louver makes the emmitance and absorptance of the radiator effectively variable. Thermal louvers are effective devices and have been used in various satellite applications, but the presence of moving parts on it makes it less reliable than heaters.

Recently, a new device that changes its surface emmitance as a function of temperature was developed (Tachikawa et al., 2000; Tachikawa et al., 2003). Called "Smart Radiation Device" (SRD), it is a ceramic thin plate which can vary its emmitance based on the ferromagnetic metal-insulator transition effect. The emmitance characteristics of these devices, are similar to the effective emittances obtained in radiators with thermal louvers, but it has the advantage of having no moving parts. On the other hand, they present a high absortivity (over 0.80), what is an undesirable characteristic for a radiator. Nevertheless, the SDR has been shown to operate successfully in space when positioned on surfaces that received no direct Solar radiation (Tachikawa et al., 2007).

With the purpose of taking advantage of the SRD emmitance characteristics, while allowing it to be used in a radiator that could face albedo or direct solar radiation, a new space radiator concept was proposed (Vlassov et al., 2006; Cuco et al., 2008). Called VESPAR (Variable Emittance SPAce Radiator), it is an aluminium device made of two stages. The internal radiator stage receives through conduction heat dissipated from equipment or payloads, and the external one rejects heat to space. While the external stage has its outer surface covered with a solar-reflective coating, as is usual to conventional space radiators (Gilmore, 1994), heat exchange between the internal and external stages is done through radiation between two surfaces covered with the SRD. Therefore, under cold conditions the radiative heat link between these surfaces is minimal, preventing the temperature of equipment or payload decrease to a level below the minimal required. On the other hand, during hot conditions, the thermal coupling is increased between the variable emittance surfaces and the temperature of the equipment or payload is kept below their maximum value limit.

The feasibility of the VESPAR concept was verified numerically using a design optimization approach, such that the radiator´s optimal design parameters (its physical dimensions) were determined to fulfill given thermal requirements in hot and cold cases scenarios (Vlassov et al., 2006). The radiator was sized using two criteria of optimization: minimize the radiator mass and the power consumption of heaters.

In order to verify experimentally the concept of VESPAR, a development model of the radiator was built, and thermal vaccum tests were performed. The radiator was built in Al 6061 with physical dimentions based on the optimized configurations obtained in Vlassov et al. (2006). Since no SRD material was available to be used in the tests, they were performed with the internal surfaces of the radiator properly set to simulate conditions of low, middle, and high radiation coupling. A low thermal coupling between the stages was obtained simply performing the tests with their internal surfaces left in bare Aluminium. A middle coupling was obtained covering the internal surface of one of the stages with Kapton® tape, while the high coupling was obtained covering the internal surface of both stages with Kapton® tape. The stages were assembled using low conductively stainless steel screws with Torlon® washers and spacers.

The rest of the paper is organized as follows: In Section 2 the VESPAR concept is briefly described. In Section 3 the manufactory of the development model is described. In Section 4, the experimental setup is presented. In Section 5 the results are shown and commented, followed by final remarks in Section 6.

2. VESPAR DESIGN CONCEPT

The concept of VESPAR is very simple. The device consists of two similar finned plates made from Al alloy as shown in Fig. 1. The upper plate is the external stage of the radiator, which has the outer surface covered with a coating commonly used in space radiators, which have a high emissivity and low solar absortivity. The bottom plate is the internal stage of the radiator and receives heat dissipated from equipment by direct contact or through a structural panel, such as the one depicted schematically in Fig. 1. The finned surfaces of both stages are covered with the SRD. The stages shall be assembled in such a way that direct thermal contact by conduction between them is avoided or minimized (for example, by the use of insulation washers), so that they exchange heat primarily by radiation. In a typical application, VESPAR would be positioned directly over the outside surface of a sattelite´s lateral panel, where one or more equipment with a high heat dissipation amplitude along the orbit were attached, as outlined in Fig. 2. In such application, Multi-Layer Insulation blankets (MLIs) provide thermal insulation of the equipment to the internal satellite environment, as well as, insulation of the lateral panel to the external environment. A heater is attached to the equipment in case additional heat is necessary to warm up it during cold cases. The thermal design configuration shown in Fig. 2, without VESPAR but with conventional radiators, and with the heaters positioned on the lateral sides of the equipment, was the thermal design solution used in CBERS 1, 2 and 2B sattellites to control the temperature of their battery packs.
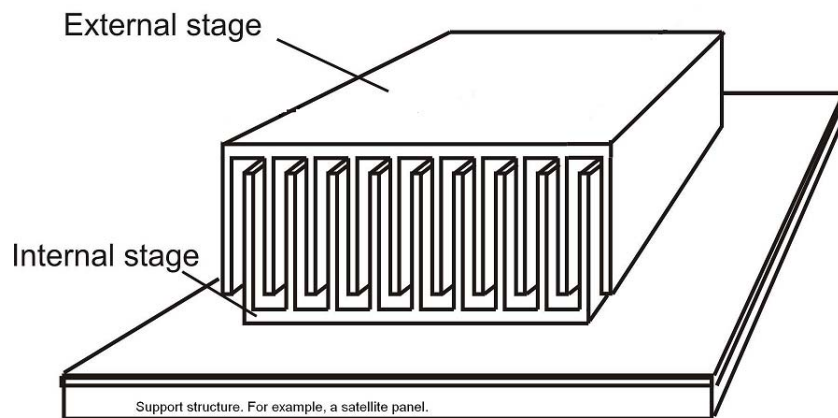
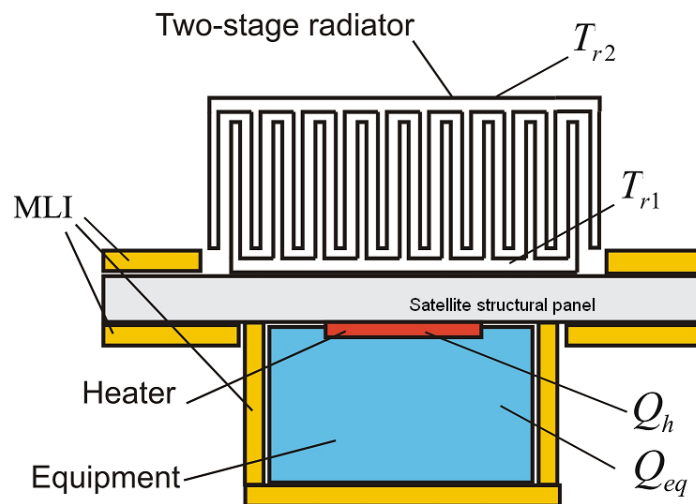Figure 1 – VESPAR physical concept. Adapted from Vlassov et al. (2006).

Figure 2 – Typical application for use of VESPAR on thermal control of a sattelite equipment. Adapted from Vlassov et al. (2006).

With the use of VESPAR instead of a conventional radiator, the need for heater power in cold conditions would be decreased or even eliminated. In the work of Vlassov et al. (2006), a reduction greater than 50 % on heater power was obtained, compared to the use of a conventional radiator, as shown in Table 1.

Table 1. Best results obtained for VESPAR design, compared to a conventional radiator, in Vlassov et al. (2006).

Type of Radiator	Q_h [W]	M_t [kg]	L [m]	H_f [cm]	δ_f [mm]	N_f
VESPAR	7	2.551	0.344	8.438	0.478	5
	7.29	2.541	0.347	8.712	0.389	5
	7.17	2.546	0.347	8.575	0.411	5
	7.52	2.536	0.338	8.137	0.389	6
Conventional	15.00	0.560	0.320	-	-	-

In Tab. 1 Q_h is the heater power, M_t is the mass of the radiator, L is its side length (a square radiator was considered), H_f is the height of the fins, δ_f is the width of the fins and N_f is the number of fins in the first stage. VESPAR´s dimensions shown in Tab. 1, were obtained using a numerical optimal design approach. An optimization algorithm was coupled to a simplified mathematical model of VESPAR, and a global search on the design space performed, in order to minimize both the radiator mass and the heater power needed to warm up the equipment in cold conditions. The design variables were the radiator´s geometric parameters shown in Tab. 1 and the heater power. The search for the optimal parameters was done considering the hot and cold cases simultaneously.

The development model of VESPAR was built based on the dimensional figures shown in Tab. 1. It is described in the following Section.

3. VESPAR DEVELOPMENT MODEL CONSTRUCTION

As mentioned in the previous Section, VESPAR development model was built based on the dimensional parameters shown in Tab. 1. Five fins were used in the first stage and its overall dimensions set to 281(l) x 215 (w) x 70.2 (h) mm. However some few changes from the design concept were introduced in the development model built: The first one was to change the angle of the fins near the edges of the radiator, so that the ones on the second stage could have a greater view factor to the external environment; another change was to manufactory the fins with variable thickness, in order to reduce the overall mass of the radiator; finally, some tabs were incorporated to the edges of both stages, so that they could be attached to each other. Six screws, with thermally insulation washers and spacers made of $Torlon_{5030}^{®}$ (conductivity k = 0.37 W/mK ($Torlon_{5030}^{®}$ data sheet)), were used to attach together the stages. In Figure 3 the overall dimensions of VESPAR development model are shown.
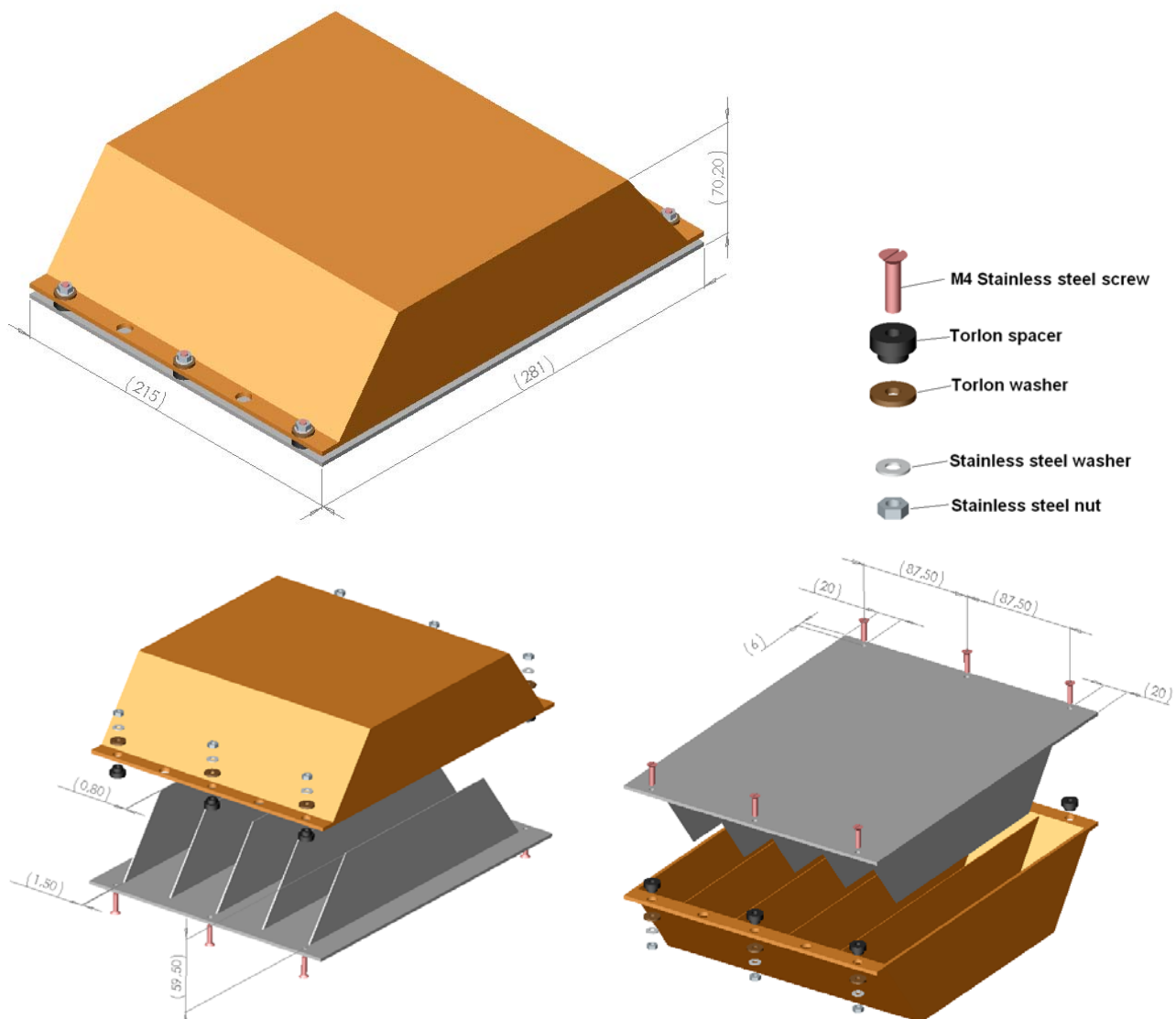

Figure 3 – VESPAR main dimensions.

Vespar development model was machined from two Al 6061 alloy blocks using a numerically controlled milling machine, as shown in Fig. 4.

Figure 4 – Manufactoring of VESPAR stages.

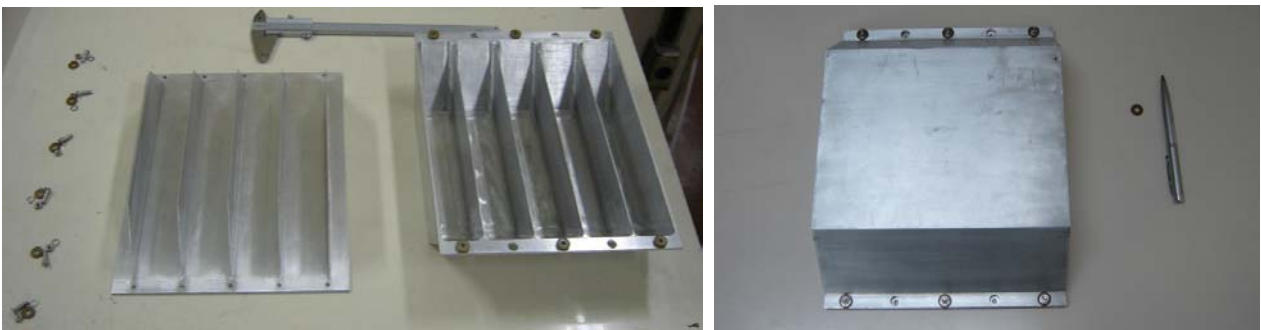In Fig. 5 views of VESPAR stages and the complete assembly are shown.

Figure 5 – VESPAR stages and assembly (without external painting).

The total mass of the radiator after fabrication was 1.545 kg.

4. THERMAL VACCUM TESTS EXPERIMENTAL SETUP

As mentioned in the Introduction, VESPAR thermal vacuum tests were designed to simulate different internal and external thermal load conditions, as well as three different thermal coupling between the stages. The internal thermal load was simulated using a skin heater (Omega HK 13034, R = 179,3 Ω). The heater and all botton surface area of the first stage was covered with a thermal insulation blanket (MLI) with 10 layers, so that almost all heat dissipated in the heater would be transfered to the botton side of the radiator´s first stage, as shown in Fig. 6.
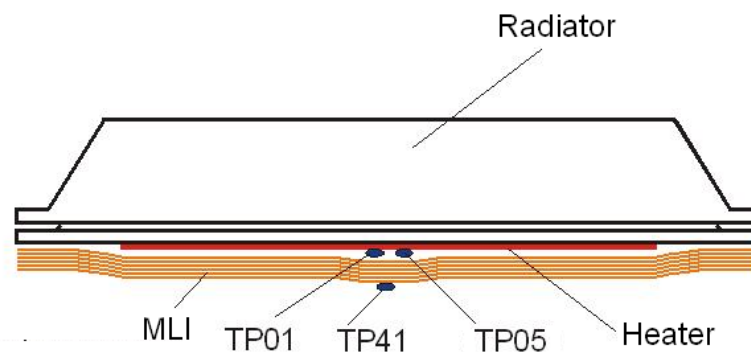

Figure 6 – Drawing of VESPAR with attached heater and MLI.

As shown in Fig. 6 three thermocouples (TPs) were used to measure the temperature on the center of the heater (TPs 01 and 05) and on the center of the outer layer of the MLI (TP41). A total of 25 TPs (Omega AWG 30) were used to measured the temperature distribution over VESPAR. The estimated accurance of the thermocouples reading (also considering uncertainty introduced by assembling procedures and the acquisition system) is ± 1.0 $^{\circ}$C. Their approximate positions are shown on Fig. 7 and 8.
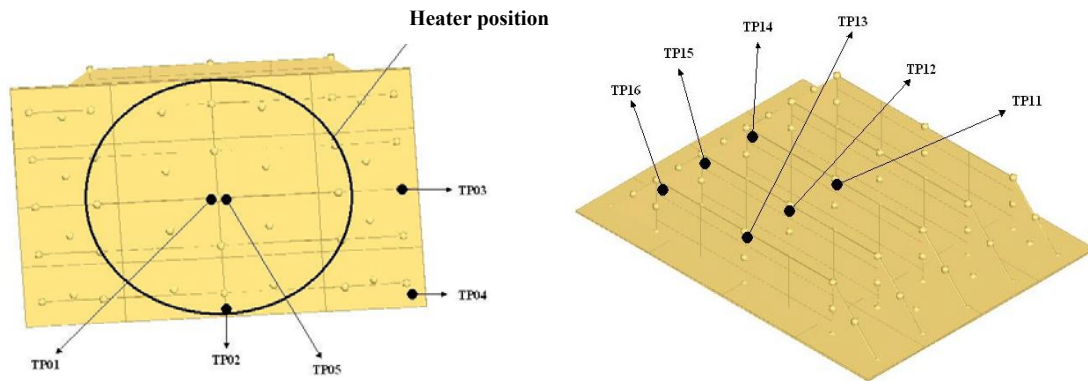
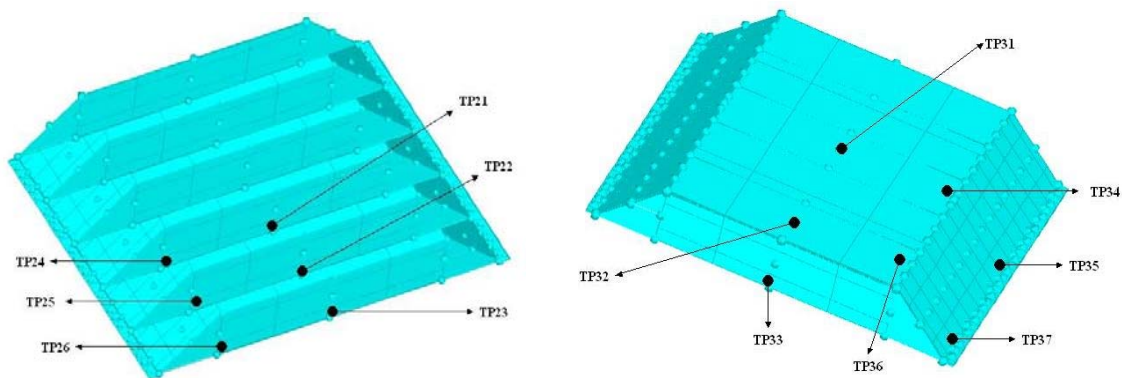Figure 7 – Thermocouple positions on first stage of VESPAR.

Figure 8 – Thermocouple positions on second stage of VESPAR.

Since in a flight model of VESPAR, the top surface of its second stage shall be covered with a coating used in conventional radiators, which has a high constant value for the emissivity, that surface in the development model was painted with a space qualified MAP-PU1 black paint. After painted black, that surface had a measured emissivity of $\varepsilon = 0.874 \pm 0.002$. A black paint was used since the development tests were performed in a environment where only infrared radiation was present, and hence there was no need to use a paint that had a low absorptivity in the solar spectrum.

To simulate three different thermal couplings between the radiator´s stages, three thermal vaccum tests were performed: i) the first one with the internal surfaces of the stages in bare aluminium, ii) the second one with the internal surface of the first stage covered with Kapton®, and iii) the third one with all internal surfaces of both stages covered with Kapton®. The measured emissivivity of the bare aluminium surface was $\varepsilon = 0.12 \pm 0.01$. After covered with Kapton®, it had $\varepsilon = 0.787 \pm 0.005$. In Figure 9 the internal surfaces of the first and second stages, covered with Kapton® and in bare aluminium respectively, and instrumented with thermocouples, are shown.
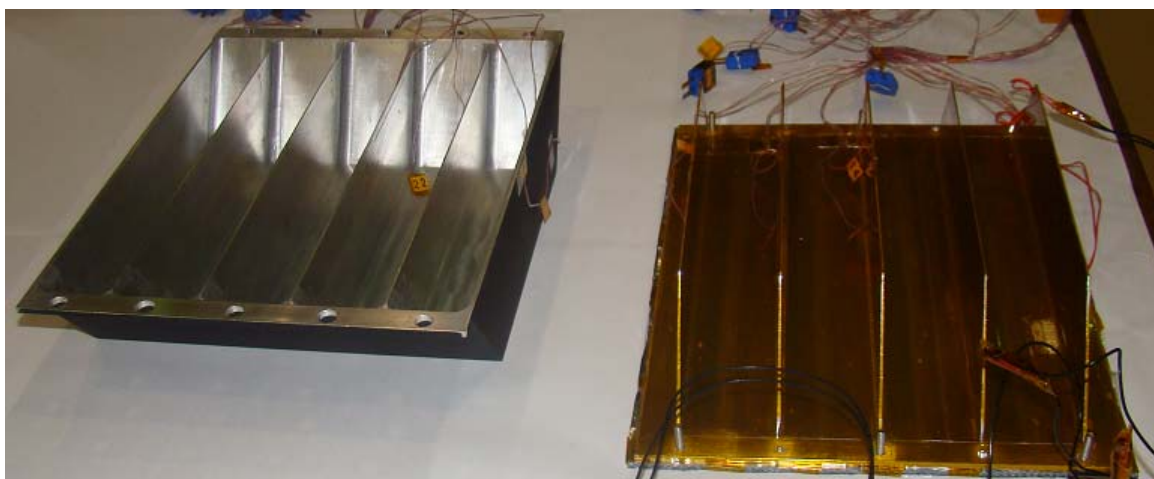

Figure 9 – Internal surfaces of first and second stage with and without Kapton® tape, respectively.

In Fig. 10 views of the radiator top and botton sides are shown.

Figure 10 – Three views of VESPAR development model. Left: Botton view of radiator without MLI (see circular heater attached to surface). Middle: Botton view of radiator botton (covered with MLI blanket). Right: Top view of second stage with TPs.

The tests were performed in two thermal vaccum chambers (TVCs) of INPE´s Test and Integration Laboratory (Laboratório de Integração e Testes – LIT). The radiator was hanged on the chamber´s shrould using two thin wires of low thermal conductivity, so that heat transfer between the radiator and the chamber´s shrould could be only by radiation. In Fig. 11 the radiator inside a TVC is shown. The pressure inside the TVCs during the tests was allways less than 10^{-6} Torr.
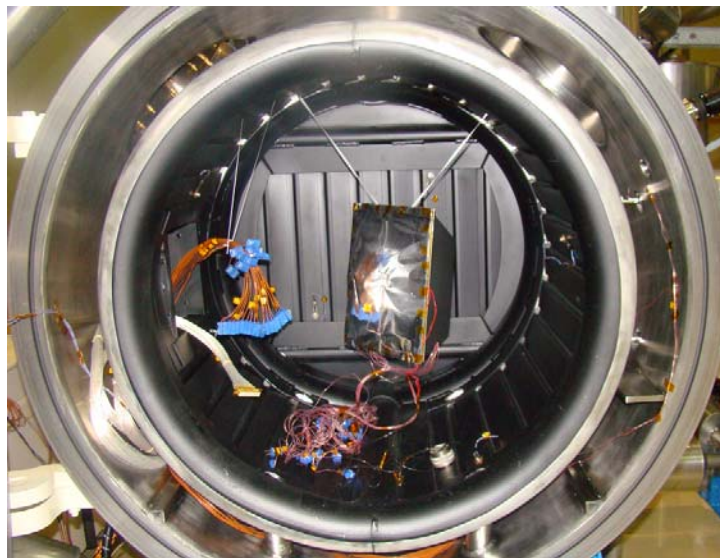

Figure 11 – VESPAR development model inside thermal vacuum chamber.

5. EXPERIMENTAL RESULTS

The tests were performed following a given nominal temperature profile for the temperature on the botton of the first stage (TP01) and for the average temperature of the chamber´s shrould (T_{CVT}). The rationale for setting the profile was: given an external thermal load (simulated by the shroud temperature, which is controlled), what would be the power dissipated in the heater (P_{heater}) necessary to keep the temperature of TP01 set on a given value? The power dissipated on the heater is adjusted by a controller, as a function of the desired temperature on TP01. The nominal temperature profile was executed in 6 phases, as followed:

1) Set T_{CVT} at -140 ^{o}C and control P_{heater} so that TP01 = -20 ^{o}C. Measure the temperature distribution over the radiator when steady state conditions are reached.
2) Change P_{heater} so that TP01 = 20 ^{o}C, keeping T_{CVT} at -140 ^{o}C. Measure the temperature distribution over the radiator when steady state conditions are reached.
3) Change P_{heater} so that TP01 = 55 ^{o}C, keeping T_{CVT} at -140 ^{o}C. Measure the temperature distribution over the radiator when steady state conditions are reached.
4) Set T_{CVT} at -80 ^{o}C and control P_{heater} so that TP01 = 55 ^{o}C. Measure the temperature distribution over the radiator when steady state conditions are reached.
5) Set T_{CVT} at -20 ^{o}C and control P_{heater} so that TP01 = 55 ^{o}C. Measure the temperature distribution over the radiator when steady state conditions are reached.

6) Set T_{CVT} at 20 ^{o}C and control P_{heater} so that TP01 = 55 ^{o}C. Measure the temperature distribution over the radiator when steady state conditions are reached.

The temperature variation of TP01, TP31, and the vacuum chamber (T_{CVT}) along the tests are shown in Fig. 12 to Fig. 14. In these Figures, are also shown, as black dots, the power dissipated on the heater, as state conditions are achieved, near the end of each test phase. The numbers in the small circles indicate the end of each phase.
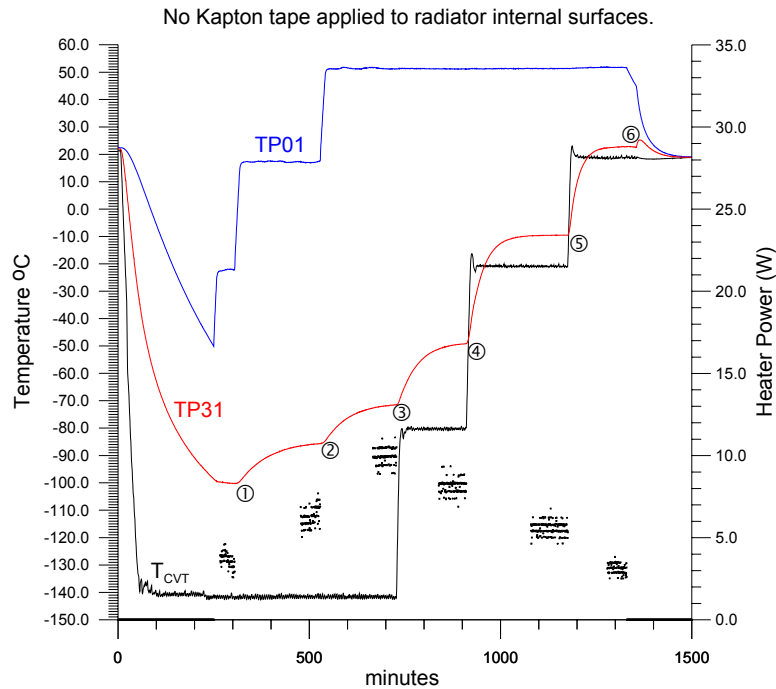
Figure 12 – Temperature and heater power variation along thermo-vacuum test, with no Kapton tape on internal surfaces of radiator.
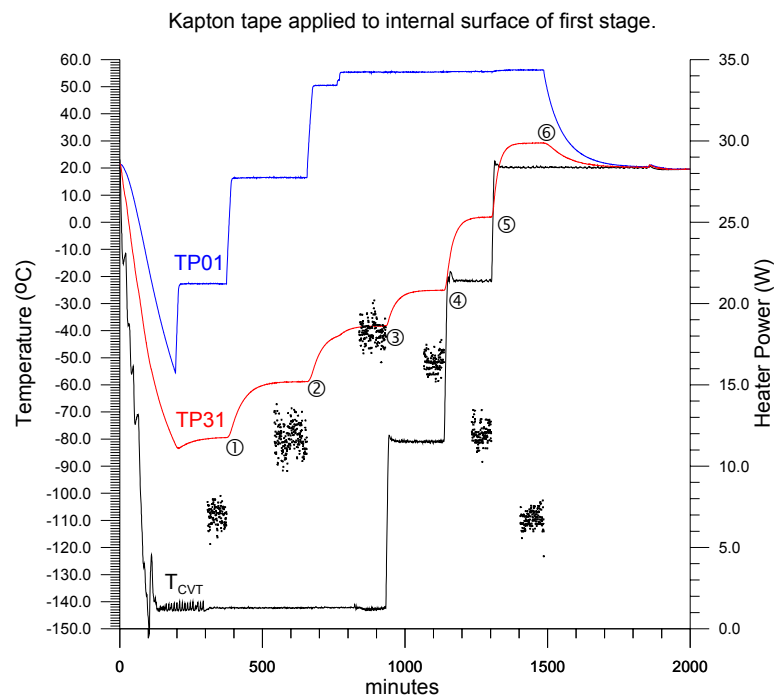
Figure 13 – Temperature and heater power variation along thermo-vacuum test, with Kapton tape applied to the internal surface of the radiator´s first stage.
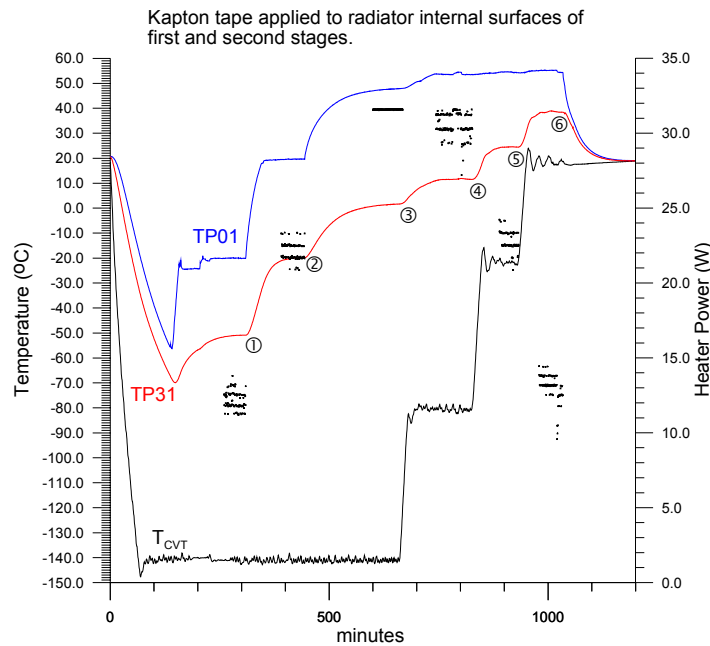
Figure 14 – Temperature and heater power variation along thermo-vacuum test, with Kapton tape applied to the internal surface of the radiator´s first stage.

In Tab. 2 to Tab. 4 the steady state temperatures obtained in each phase, the effective thermal coupling between the two stages (G) and the average power (Q_{h_VESPAR}) dissipated on the heater in these conditions, are shown. On the Tables is also shown the power ($Q_{h,CONV}$) that would be needed at the heater if a conventional radiator instead of VESPAR was used on the tests. The conventional radiator uses the same base area as VESPAR.

Table 2 – Value of test parameters for radiator with internal surfaces of both stages in bare aluminium.

Test Phase	1	2	3	4	5	6
T_{CVT}	-142.0	-142.0	-142.0	-80.3	-21.0	18.8
TP01 (^{o}C)	-22.2	17.2	51.3	51.3	51.3	51.8
TP31 (^{o}C)	-100.2	-84.8	-71.8	-50.8	-9.8	22.5
G (W/C)	0.047	0.062	0.081	0.080	0.092	0.108
Q_{h_VESPAR} (W)	3.7	6.3	10.0	8.2	5.6	3.17
$Q_{h,CONV}$ (W)	12.7	23.6	37.3	33.6	24.4	13.5

Table 3 – Value of test parameters for radiator with internal surface of first stage covered with Kapton tape.

Test Phase	1	2	3	4	5	6
T_{CVT}	-142.0	-142.0	-142.0	-81.0	-21.8	20.0
TP01 (^{o}C)	-23.0	16.5	55.0	55.0	55.0	56.0
TP31 (^{o}C)	-79.9	-59.0	-38.5	-25.0	1.5	29.0
G (W/C)	0.12	0.16	0.20	0.21	0.23	0.25
Q_{h_VESPAR} (W)	7.1	11.8	18.3	16.5	12.1	6.8
$Q_{h,CONV}$ (W)	12.5	23.3	39.1	35.4	26.3	15.1

Table 4 – Value of test parameters for radiator with internal surfaces of both stages covered with Kapton tape.

Test Phase	1	2	3	4	5	6
T_{CVT}	-141.0	-141.0	-141.0	-81.0	-21.2	18.0
TP01 (^{o}C)	-20.0	19.5	47.9	53.5	54.4	54.8
TP31 (^{o}C)	-51.0	-20.2	1.8	11.3	24.5	38.5
G (W/C)	0.40	0.56	0.69	0.73	0.77	0.81
Q_{h_VESPAR} (W)	12.3	22.3	31.8	30.8	23.1	13.2
$Q_{h,CONV}$ (W)	13.2	24.3	35.7	34.7	25.9	15.2

The results presented in Fig. 12 to Fig. 14 and Tab. 2 to Tab. 4 confirm the expectation that great savings on heater power can be obtained with VESPAR in cold conditions. The effective coupling between the radiator stages (G) is in

the range from 0.047 to 0.81 (W/C) . The average power saving, defined as the average ratio between $Q_{h,CONV}$ and Q_{h_VESPAR} for all phases along a test profile, achieved a maximum value of 3.93. It is a significant figure, however obtained under the optimistic assumption that the emissivity of the internal surfaces of VESPAR covered with SRDcould vary in the range between 0.12 and 0.787. The variation of emissivity of the SRD is lesser than that (Tachikawa 2000, 2003) and therefore a lesser saving is expected in a flight model of VESPAR.

The temperatures measured in the experiments will be used to adjust VESPAR mathematical model and a remake of its design will be performed, in order to reach a maximum figure on heater power saving, taking into account experimental thermal parameters of VESPAR and the SRD emissivity properties.

6. FINAL REMARKS

The feasibility of VESPAR concept was proved experimentally through thermal vacuum tests with application of different coatings on the internal surfaces of the radiator. Main parameters of the radiator were obtained experimentally, which will be used for the benchmarking of the mathematical model. The maximum average power saving obtained in the tests was 3.93. This high figure is a good prospect for what would be obtained with VESPAR using SRD on its internal surfaces. This will be evaluated in a further work with the adjusted mathematical model of VESPAR.

7. ACKNOWLEDGEMENTS

The authors would like to thank engineer Pedro Cândido for the help in the preparation of the experimental setup and realization of the test cases.

8. REFERENCES

Cuco, A.P.C., De Sousa, Vlassov, V.V. e Silva Neto, A.J. "Multi-Objective Design Optimization of a New Space Radiator". Proceedings of International Conference on Engineering Optimization – EngOpt2008, Rio de Janeiro, 01-05 June 2008.
Gilmore D.G. (Editor), 1994, "Satellite Thermal Control Handbook", The Aerospace Corporation Press, California, United States.
Karan, R. D., 1998, "Satellite Thermal Control for Systems Enginees", Vol 181, Progress in Astronautics and Aeronautics, 286 p.
Muraoka, I., Sousa, F.L., Parisotto, W.R. and Ramos, F.M., 2001, "Numerical and Experimental Investigation of Thermal Louvers for Space Applications", Journal of the Brazilian Society of Mechanical Sciences, Vol. XXIII, No. 2, pp. 147-153.
Tachikawa S., Ohnishi A., Shimazaki, K., Kosaka, M., Mori, T. and Ochi, A., 2000, "Design and Ground test Results of a Variable Emittance Radiator", Proceeding of the 30th ICES - International Conference on Environmental Systems, Toulouse, France, July, Paper SAE 2000-01-2277.
Tachikawa S., Ohnishi A., Shimakawa Y., Ochi A., Okamoto A. and Nakamura Y., 2003, "Development of Variable Emittance Radiator Based on a Perovskite Magnese Oxide", Journal of Thermophysics and Heat Transfer, Vol. 17, No 2, April-June 2003, pp. 264-268.
Tachikawa S., Ohnishi A., Nakamura Y., Okamoto A., 2007, "In-Orbit Thermal Performance of a Smart Radiation Device", Proceeding of the International Conference on Environmental Systems, Chicago, USA, July, Paper SAE 2007-01-3125.
Vlassov, V. V., Cuco, A. P. C., Sousa, F. L. e Silva Neto, A. J., "Design Optimization of two-stage radiator with variable emittance: analysis of concept feasibility", Proceedings of the 11th Brazilian Congress of Thermal Sciences and Engineering (CDROM), ENCIT 2006, Curitiba, PR, 5 a 8 de Dezembro de 2006.

9. RESPONSIBILITY NOTICE

The authors are the only responsible for the printed material included in this paper.